# Effect of LINC00320 Regulating the Expression of PLEKHA1 through the Transcription Factor MYC in Glioma Cell Proliferation, Migration, Invasion and Apoptosis In vivo and In vitro

**Jianyong Ji**
Liaocheng People's Hospital
**Pengfei Xue**
Liaocheng People's Hospital
**Juan Zheng**
Liaocheng People's Hospital
**Rongrong Li**
Dongchangfu People's Hospital
**Jinyue Fu**
Dongchangfu People's Hospital
**Zhaohao Wang**
PKU Care Luzhong Hospital
**Xin Li** ( drlixin88@126.com )
Liaocheng People's Hospital https://orcid.org/0000-0002-3070-352X

**Research**

**Keywords:** LINC00320, MYC, PLEKHA1, Transcription factor, Glioma

**Posted Date:** April 1st, 2021

**DOI:** https://doi.org/10.21203/rs.3.rs-306949/v1

# Abstract

**Aim:** This study was carried out to explore the mechanism and function of LINC00320 in the development of glioma by regulating PLEKHA1 expression through transcription factor MYC.

**Methods**: By searching LINCDISEASE database and through difference analysis of glioma chip, glioma related lncRNAs were screened, and lncRNA-transcription factor-mRNA triplet was predicted through lncMAP database. The expressions of LINC00320 and PLEKHA1 were detected in glioma and normal controls, followed by the detection of the proliferation, invasion, migration, and apoptosis of glioma cells by using CCK-8 method, Transwell assay, and flow cytometry, respectively. In addition, the expression patterns of MMP9 and cleaved-Caspase 3 were detected with Western Blot. Furthermore, the possible mechanism of LINC00320 was predicted in gliomas by LncMAP. RIP assay was performed to verify the interaction between LINC00320 and MYC, and ChIP assay was applied to validate the binding of MYC and PLEKHA1 promoter. The existence of binding site between MYC and PLEKHA1 promoter were determined by dual luciferase reporter gene assay. Lastly, *in vivo* test was conducted by using nude mice as the objects of study for verification of the results obtained by *in vitro* tests.

**Results**: LINC00320 was found to be significantly down-expressed in glioma, and patients with low expression levels of LINC00320 exhibited an even worse prognostic outcome. Over-expression of LINC00320 in glioma cells brought about a significant reduction in cell proliferation, migration, invasion, and promoted apoptosis. There was a significant decrease in the protein expression of MMP9 but remarkable increase in that of cleaved-Caspase 3 after LINC00320 over-expression. LncRNA-transcription factor-mRNA triplet prediction showed that LINC00320 regulated the expression of PLEKHA1 through MYC. RIP assay demonstrated that MYC could significantly enrich LINC00320, Chip assay showed that MYC bound with the PLEKHA1 promoter, and dual luciferase reporter gene assay further confirmed the presence of binding site between MYC and PLEKHA1 promoter. Cell function experiment verified that PLEKHA1 could reverse the effect of LINC00320 over-expression.

**Conclusion:** Over-expression of LINC00320 can attenuate the binding of MYC with PLEKHA1 by recruiting MYC, and ultimately inhibit the proliferation, migration and invasion, and promote the apoptosis of glioma cells.


# Background

Gliomas are the most common malignancy of the brain, accounting for about 50% of primary brain tumors [1, 2]. Unfortunately, the median survival of patients with gliomas is extremely low despite the advent of surgical regimens and postoperative adjuvant radiotherapy and chemotherapy [3, 4]. At present, it is imperative to improve the therapeutic effect of gliomas and reduce the recurrence considering the limited clinical use of various therapeutic approaches for gliomas [5]. In recent decades, rapid development in the field of tumor cell research has been greatly attributed to the gradual elucidation of functions of transcription factors. Transcription factors are proteins that possess the ability to bind to

specific DNA sequences and regulate gene transcription [6-8]. Several transcription factors can also contribute to tissue- or cell-type-specific gene expressions, and are thus involved in the development of malignancies. Moreover, some transcription factors, such as Octamer-binding transcription factor (Oct4), B-lymphoma Moloney murine leukemia virus insertion region-1 (Bmi1) and Nanog, have been found to be implicated in the early development of embryo, which not only regulate the maintenance of normal cell attributes, but also play a vital role in the maintenance of tumor cell biological characteristics [9-11]. Also, the gene product of MYC, especially c-MYC, also plays an important role in the induction of apoptosis [12]. MYC is one of the well-known transcription factors that serves as an oncogene to promote the genesis of various human tumors [13], and recent studies on its expression and function have further highlighted its therapeutic opportunities [14-16]. Furthermore, studies have uncovered that MYC can mediate the expressions of both protein and non-coding RNA to regulate cell growth, proliferation, differentiation and drug resistance, etc. [17, 18]. However, it is still unclear with respect to the molecular and genetic mechanisms of MYC in patients with glioma.

Long noncoding RNAs (lncRNAs) are a class of transcribed RNA molecules of >200 nucleotides in length [19-22]. LncRNAs are capable of modulating the expressions of target genes at transcriptional, post-transcriptional, and epigenetic levels, not encoding proteins [23, 24]. More importantly, a large number of studies have demonstrated that lncRNAs confer significant functions in various biological steps such as cell cycle processes, cell differentiation, etc. [25-27]. Numerous lncRNAs such as lncRNA LOC441204 and PVT1 are known to play multi-roles in glioma cells acting as oncogenes or tumor suppressors. Furthermore, previous studies also support the important roles of numerous oncogenic and anti-oncogenic lncRNAs in the development of gliomas [28-31]. Another such lncRNA, LINC00320, was previously indicated to be human brain-specific and highly-expressed in the cortical white matter [32]. Moreover, a recent study showed that LINC00320 as a tumor suppressive lncRNA, was down-regulated in glioma tissue and suppressed the proliferation of glioma cells by inhibiting the activation of Wnt/β-catenin signaling pathway, and further proposed a novel axis of HMGB1/LINC00320/β-catenin in glioma [33]. However, there are no such reports about LINC00320 involvement in glioma, and was thus chosen as the prime focus lncRNA for a more comprehensive and systematic investigation. Meanwhile, PH domain-containing family A member 1 (PLEKHA1), also known as TAPP1, is known as a member of the superfamily of proteins containing the PH domain [34]. Previous evidence has documented that PLEKHA1 can bind with PtdIns(3,4)P2 specifically through its C-terminal PH domain [35]. So far, there is a dearth of studies relating its role in the regulation of cell migration. More pressingly, there is a lack of evidence investigating the relationship between LINC00320, PLEKHA1 and MYC, which was hypothesized to be correlated interactively in our study and would be explored subsequently. In view of the above interpretations, the present study was carried out to explore the mechanism and function of LINC00320, the roles of PLEKHA1 and MYC as well as their relationship in the development of glioma.

# Materials And Methods

### Bioinformatic Analysis

Firstly, lncRNAs related to glioma were obtained by retrieving LINCDISEASE database (http://www.rnanut.net/lncrnadisease/index.html), and finally 142 Experimental and Experimental/Predicted lncRNAs were screened after the exclusion of duplicate items. Subsequently, GEO database (https://www.ncbi.nlm.nih.gov/geo/) was searched to obtain a microarray dataset of glioma, GSE15824, which comprised of 2 normal samples and 12 tumor samples. Differential analysis was then performed using the “limma” package of R language with normal samples as the control, while |logFC|>2 and p value<0.05 were regarded as the screening criteria for the differential expressed genes. Furthermore, the GEPIA database (http://gepia2.cancer-pku.cn/#index) was explored to the expression patterns of LINC00320, MYC and PLEKHA1 in relation to glioma in TCGA. Additionally, the downstream transcription factors and regulatory gene triplets of LINC00320 in low-grade glioma were predicted by searching the lncMAP database (http://bio-bigdata.hrbmu.edu.cn/LncMAP/survival.jsp).

## Sampling

A total of 60 cases of glioma were confirmed by pathology and collected from January 2013 to January 2014 for inclusion in the current study. The eligible patients received operations for the first time, including 38 males and 22 females (aged 46-67 years old; average age of 55.17 years old). Of the enrolled 60 cases, 31 cases were in stage I+II, 29 cases in stage III; 21 cases with KPS ≥80 points, and 39 cases with KPS <80 points. The exclusion criteria in our study omitted patients with severe metabolic system diseases, patients complicated with other malignant tumors, patients with incomplete clinical data, and patients with severe heart, kidney and lung dysfunction; and those with severe cognitive impairment. In addition, 35 cases of normal brain tissue resected by internal decompression operation in patients with severe brain injury were taken as the control group, and none of the aforementioned patients underwent radiotherapy and chemotherapy prior to operation. The follow-up lasted for 5 years, till January 2019, and was performed by using telephone or review. The overall survival (OS) rate of enrolled patients was calculated, and it was defined as the time from the randomization of enrollment to the death of patients for any reason. The OS of each group was observed and recorded for 5 years. At the end, during the follow-up period of 3-60 months, 7 patients were lost to follow-up, with a calculated follow-up rate of 88.33%.

## Cell Culture and Transfection

The human microglia cell line CHME-5, glioma cell line SHG-44, U251 and BT325 cells was purchased from the Cell Resource Center of Shanghai Institute of Life Sciences, Chinese Academy of Sciences. CHG5 cells were purchased from Shanghai Qincheng Biotechnology Co., Ltd. SHG-44, The obtained cells were cultured in RPMI 1640 (w/o Hepes) medium containing 10% fetal bovine serum, 100 U/mL penicillin and 100 mg/mL streptomycin in a humidified incubator with 5%$CO_2$ at 37 ℃.

According to the experimental requirements, SHG-44 cells at the logarithmic phase of growth were transfected, among which the lentivirus over-expression vectors were constructed according to the sequence information of LINC00320 and MYC. Subsequently, LINC00320 stable over-expression

sequence(F: 5'-AATTTTACACATCTGTCTATACACAT-3'; F: 5'-TCAGTTGTCACTAAAGTAAGCAATGT-3') and MYC over-expression sequence (F: 5'-TTCCTGTTGGTGAAGCTAACGTTGAGGGGCAT-3'; F: 5'-TCAACTGTTCTCGTCGTTTCCGCAACAAGTCC-3') were transfected to the PLV vector. Based on the information of PLEKHA1, the specific siRNA sequence (SS sequence: GGGTAAATGTGTTAAACAA, and AS sequence: TTGTTTAACACATTTACCC) and its control sequence (SS sequence: GGUGGUGUGUGUCUGUAGU , and AS sequence: ACUACAGACACACACCACC) targeting human PLEKHA1 gene were connected to the PLKO-Puro vector. After correct sequencing, the plasmid was co-transfected with psPAX2 and pMD2.G (Addgen, USA) into the HEK293T cells. Supernatant of the culture medium containing lentivirus particles was collected to infect SHG-44 cells for screening the stable cell lines.

### qRT-PCR Test

Total RNA content was extracted using Trizol kits (Invitrogen, California, USA), and PrimeScript RT kits (rr037a, Takara, Japan) were employed to reverse transcribe the RNA into cDNA. The system was 10ul and was operated in accordance with the manufacturer's instructions. The reaction conditions were as follows: 37℃, 15 min×3 times (reverse transcription reaction), followed by processing at 85℃ for 5 s (reverse transcriptase inactivation reaction). The reaction solution was selected for the fluorescent quantitative PCR to perform fluorescent quantitative PCR according to the instruction of SYBR®Premix ExTaqTM kit (RR820A, TaKaRa). The reaction system was 50 μL in amount, including 25 μL of SYBR®Premix Ex TaqTM(2×), 2 μL of PCR upstream primer, 2 μL of PCR downstream primer, 1 μL of ROX Reference Dye (50×), 4 μL of DNA template, and 16 μL of $ddH_2O$. Real-time fluorescence quantitative PCR system (ABI 7500, ABI, Foster City, CA, USA) was then carried out for fluorescence quantitative PCR, and the reaction conditions were as follows: pre-denaturation at 95℃ for 10 min, denaturation at 95℃ for 15 s, annealing at 60℃ for 30 s (40 cycles), and extension at 72℃ for 1 min finally. With β-actin serving as the internal reference, the relative expression of each target gene was calculated using the $2^{-\Delta\Delta Ct}$ method according to the formula of $\Delta\Delta Ct=\Delta Ct_{\text{experimental group}}-\Delta Ct_{\text{control group}}$ and $\Delta Ct=Ct_{\text{target gene}}-Ct_{\text{internal reference}}$, and each experiment was repeated three times. Relevant primers were designed by Sangon Biotech (Shanghai) Co., Ltd. (Table 1).

### Western Blot

Total protein content in tissues or cells was extracted from RIFA lysate of SF, incubated on ice for 30 min, and centrifuged at 4 ℃ for 10min (8,000g) to obtain the supernatant. BCA kits were employed to detect the total protein concentration. Next, 50 μg protein was dissolved in 2 × SDS sampling buffer and boiled at 100℃ for 5 min. The above samples were then subjected to SDS-PAGE gel electrophoresis, and the proteins were transferred to PVDF membrane using the wet-transfer method, followed by sealing with 5% skim milk powder at room temperature for 1 h. After that, PVDF membrane was incubated overnight at 4℃ with the rabbit anti-MMP9 antibody (dilution ratio of 1:1000, ab38898, abcam, Cambridge, UK) and rabbit anti-cleaved-Caspase-3 antibody (dilution ratio of 1:500, ab49822, abcam, Cambridge, UK), with β-actin (dilution ratio of 1:2000, ab227387, abcam, Cambridge, UK) as the internal reference. After TBST

washing three times (10min each), PVDF membrane was incubated with the HRP labeled goat anti-rabbit IgG H&L (HRP) (dilution ratio of 1:2000, ab97051, abcam, Cambridge, UK) for 1 h, followed by TBST washing. Same amounts of solution A and solution B solution were taken from the ECL fluorescence detection kit, mixed in dark conditions, and dropped onto the film for imaging in an gel imager. Photography was carried out with the Bio-Rad image analysis system (Bio-Rad company, USA), and associated with analysis using the Quantity One v4.6.2 software. The gray value of corresponding protein bands/β-actin protein bands represented the relative protein content. The experiment was repeated three times to obtain the mean value.

### Immunofluorescence

Subcellular localization of LINC00320 and MYC in the SHG-44 cell line was identified using immunofluorescence techniques. A cover glass was placed on a 6-well culture plate, followed by inoculation of SHG-44 cells, and then cultured for 1 d to make the cell fusion rate about 80%. The slides were taken out and washed with PBS. Then, 1 mL of 4% paraformaldehyde was added for cell fixation at room temperature, followed by the addition of 250 μL of pre-hybridization solution containing LINC00320 and MYC probes to incubate at 42℃ for 1 h after treatment with protease K (2 μg/mL), glycine and acetylate reagent. Next, the pre-hybridization solution was absorbed and 250 μL of hybridization solution containing probe (300 ng/mL) was added for hybridization overnight at 42℃. After PBST rinsing (×3 times), DAPI (dilution ratio of 1:800) staining solution diluted with PBST was added to stain the nucleus, followed by transferring to the 24-well culture plate, staining for 5 min; washing with PBST (×3 times), 3 min each time. Finally, five different fields of vision were observed and photographed under a fluorescence microscope (Olympus, Japan) after anti-fluorescence quenching agent for sealing.

### CHIP Assay

SHG-44 cells from each group was treated with formaldehyde for 10 min to produce DNA protein cross-linking. An ultrasonic crusher was then employed and set to break the chromatin into fragments by 10s in 15 cycles, with time interval of 10s. After centrifugation at 4℃ for 10 min, the supernatant was collected and divided into two tubes. Negative control antibody of IgG of normal mice and specific antibody anti-MYC (#18583S, dilution ratio of 1:100, Cell Signaling Technology Inc.) of the target protein were added and incubated at 4℃ overnight for full binding. Next, the DNA protein complex was precipitated with Protein Agarose/Sepharose, followed by centrifugation (12,000g) for 5 min, and the supernatant was discarded. After washing the non-specific complex, the cross-linking was removed overnight at 65℃, and DNA fragments were extracted and purified with phenol/chloroform. Finally, the binding of MYC to the promoter region of PLEKHA1 was detected by means of PCR with PLEKHA1 using specific primers.

### RIP Assay

The binding of LINC00320 to MYC was detected using RIP kits (millipore, USA). After rinsing the SHG-44 cells with pre-cooled PBS, cells were lysed with RIPA lysate (P0013B, Beyotime) of equal volume in an ice bath for 5 min after discarding the supernatant, followed by centrifugation at 4℃ for 10 min (12,000 g).

A portion of the cell extract was taken out as input and a part of that was incubated with antibody for co-precipitation. As for the specific steps, each co-precipitation reaction system was washed with 50 μL magnetic beads and then re-suspended in 100 μL RIP Wash Buffer, and 5 μg antibody was added to incubate for binding. After cleaning, the bead antibody complex was re-suspended in 900 μL RIP Wash Buffer and incubated overnight with 100 μL cell extract at 4 ℃. Next, the sample was placed on the magnetic base to collect the bead-protein complex. After digestion with protease K for the sample and input, RNA content was extracted for subsequent PCR detection. The antibody used for RIP was anti-MYC, which was mixed at room temperature for 30 min, and IgG was used as negative control.

### Dual Luciferase Reporter Assay

The binding sites of the promoter region of PLEKHA1 with MYC were predicted by website analysis through lncMAP website. PLEKHA1 promoter region was transfected into pGL3-Basic vector (Promega) to serve as the recombinant vector of PLEKHA1-WT. Meanwhile, the MYC binding site mutation of PLEKHA1 was constructed into the pGL3-Basic vector (Promega) to serve as the recombinant vector of PLEKHA1-MUT. The correctly sequenced luciferase reporter plasmid WT and MUT were then transfected into HEK-293T cells with MYC respectively. After 48 h of transfection, luciferase activity was detected by collecting and cleaving cells. In accordance with the instructions of dual luciferase reporter assay kit, the cells were rinsed with PBS and lysed in 200 μL lysate for 15 min. Luciferase activity was measured at 560 nm using Firefly Luciferase Reporter Gene Assay kits (RG005, Beyotime, China) and a microplate reader. Each experiment was repeated three times to obtain the mean value.

### CCK-8 Detection of Cell Growth Curve

The transfected SHG-44 cells were digested and re-suspended. Next, the cell density was adjusted to $1\times10^5$ cells/mL and inoculated in 96-well plate with 100μL per well, and allowed to culture overnight. The following day, the cells were treated according to the instructions of CCK-8 kit (Beyotime, Shanghai, China). The cell viability was detected using the CCK-8 method at 24, 48, 72, 96 h after inoculation. An amount of 10μl CCK-8 detection solution was added to each test, and placed in the incubator for 4 h. The absorbance of CCK-8 at wavelength of 450 nm was detected using a microplate reader to plot the growth curve.

### Transwell Assay

Matrigel preserved at - 80 ℃ was taken out and allowed to melt into the liquid state overnight at 4 ℃. Next, 200 μL of Matrigel was added to 200 μL of serum-free medium at 4℃ and mixed well to dilute the matrix gel. An amount of 50 μL was then added to the upper chamber of each Transwell plate, placed into the incubator, and incubated for 2-3 h until solidification of glue. After digesting and counting, the cell suspension was prepared with serum-free medium. Then, 200 μL of cell suspension was added to the upper chamber of each well, and 800 μL of medium containing 20% FBS was added to the lower chamber, which was placed in an incubator at 37 ℃ for 20~24 h. Afterwards, the Transwell plate was taken out, rinsed twice with PBS, soaked in formaldehyde for 10 min, and then washed thrice with water.

After 0.1% crystal violet staining, the cells were placed at room temperature for 30 min, rinsed twice with PBS and wiped off with a cotton swab. Finally, the cells were observed, photographed and counted under an inverted microscope. Transwell migration experiment required no matrix glue, and the incubation time was 16 h. Cells from at least four microscope areas were randomly selected to count. Each experiment was repeated three times to obtain the mean value.

### Flow Cytometry

After 48 h of transfection, cells were digested with 0.25% trypsin (free of EDTA) (YB15050057, Yu Bo Biotech Co., Ltd., Shanghai, China) and collected in a flow tube, centrifuged, and the supernatant was discarded. Next, the cells were rinsed thrice with PBS and centrifuged to discard the supernatant. According to the instructions of Annexin-V-FITC cell apoptosis detection kit (K201-100, Biovision, USA), Annexin-V-FITC, PI, HEPES buffer solution were prepared into an Annexin-V-FITC/PI staining solution at a ratio of 1:2:50. Cells at the density of $1\times10^6$ cells/mL were re-suspended every 100 μL of staining solution, and were evenly mixed by shaking. After incubation at room temperature for 15 min, 1 ml of HEPES buffer solution (PB180325, Procell, China, China) was added, and the cells were again evenly mixed by shaking. FITC and PI fluorescence were detected by 525 nm and 620 nm band-pass filters excited at 488 nm for the detection of cell apoptosis. Each experiment was repeated three times to obtain the mean value.

### Tumorigenesis Experiment in Nude Mice

A total of 10 BALB/c male nude mice (aged 4-5 weeks; weighing about 18-22 g) were obtained from the Shanghai SLAC Laboratory Animal Co.,Ltd for *in vivo* experimentation. The lentivirus vector was constructed by over-expression of LINC00320 to obtain SHG-44 cell line with stable expression of LINC00320 and its empty vector. After cell concentration adjustment to $1.0\times10^6$/mL, 20 μL of cell suspension was taken and inoculated into the subcutaneous tissue of the abdomen of nude mice, and tumorigenesis was observed every 5 days. The maximum diameter ‘a’ and minimum diameter ‘b’ of transplanted tumor were measured using Vernier calipers, followed by calculating the weight and volume of tumor (TV) according to the formula $TV=1/2\times a\times b^2$. After 30 d, nude mice in each group were euthanized, the tumor tissue was extracted, and the tumor mass was weighed with a balance. The measurement was repeated three times in each group. All the above experimental animals were approved by the Animal Care and Use Committee (Ethics Committee Approval No.201306005). Processing of the animal experiment in this study conformed to the management and usage principles of local experimental animals.

### Immunohistochemistry

Paraffin embedded sections of mice were dewaxed and hydrated for 10 min, and xylene I and II were used to dewax for 10 min respectively, followed by dehydration with gradient alcohol and two PBS rinses (5 min each time). After soaking with 3% $H_2O_2$ for 10 min and another two times of PBS rinsing (5 min each time), high-pressure antigen repair (Beyotime, China) was conducted for 90s, followed by cooling at room

temperature and section rinsing with PBS. Next, 5% BSA blocking solution was added for incubation at 37℃ for 30 min, followed by the addition of 50μl of VEGF rabbit monoclonal antibody (dilution ratio of 1: 250, ab32152, abcam, Shanghai, China) and CD31 rabbit monoclonal antibody (dilution ratio of 1:50, ab28364, abcam, Shanghai, China) in a refrigerator at 4℃ overnight. After PBS rinsing for 2min, 50 μL HRP labeled goat anti-rabbit secondary antibody (dilution ratio of 1:10000, ab205718, abcam, Shanghai, China) was added for incubation at 37℃ for 30 min. With the addition of SAB working solution, DBA (Fuzhou Maixin Biotechnology Development Co., Ltd.) was used for development, followed by re-staining with hematoxylin for 5min, observation and photography under optical microscope (XSP-36, Bostar Optical Instruments Co., Ltd., Shenzhen, China). Five high power fields (×200) were randomly selected for each section, with 200 cells in each field, with the purpose of analyzing the ratio of positive cells [36].

### Statistical Analysis

Statistical analyses were performed using the SPSS 21.0 software (IBM SPSS statistics, Chicago, IL, USA). Measurement data were expressed by mean ± standard deviation. Normal tissues and cancer tissue data were evaluated by paired t-test; data between groups were compared by unpaired t test; and that among multiple groups were compared by one-way analysis of variance (ANOVA) and Tukey's post-hoc test. Two-way ANOVA was applied for cell activity at different time points, and repeated ANOVA was used for tumor volume at different time points. Bonferroni correction was made in post-hoc tests. Pearson correlation analysis was performed for correlation between the two indexes. Kaplan-Meier test was used to analyze the survival of patients with high and low expression, and Log-rank test adopted for difference comparison. A value of $p < 0.05$ was regarded statistically significant.

## Results

### LINC00320 Involved in the Development of Glioma

The GSE15824 dataset with glioma expression patterns was obtained by retrieving the GEO database. Subsequent difference analysis of the gene expression between normal samples and glioma samples in the dataset reared a total of 657 significantly different expressed genes (Figure 1A). Additionally, 142 glioma related lncRNAs were obtained from LNCDISEASE database to explore the mechanism of lncRNA regulating disease through transcription factors in glioma. Moreover, the lncMAP database was searched to obtain the triplet data of lncRNA-transcription factor-mRNA in lncMAP database. Microarray analysis was then performed to obtain the intersection of lncRNA in the LNCDISEASE database and that in the triplet within lncMAP database (Figure 1B), with one lncRNA of LINC00320 obtained finally. In addition, microarray analysis indicated that the expression of LINC00320 was significantly downregulated in glioma (Figure 1C). Meanwhile, the expression patterns of LINC00320 in glioma in TCGA and GTEX databases were analyzed by GEPIA database (Figure 1D), with a similar down-regulated expression trend observed in the tumor. In order to further determine whether LINC00320 was involved in the development of glioma, qRT-PCR was applied to detect the expression levels of LINC00320 in the collected glioma tissues and controls. It was found that the expression levels of LINC00320 in human gliomas were

significantly lower than those in non-tumor brain tissues ($p$<0.05) (Figure 1E). According to the average expression level of LINC00320 in gliomas (0.414), the high expression group (n =31) and low expression group (n =29) were established to analyze the relation between high and low expressions of LINC00320 and the clinicopathological characteristics of patients. LINC00320 expression was found to be not significantly correlated with age, gender and recurrence, while showing correlation with tumor size, stage, WHO grade and KPS score ($p$<0.05) (Table 2). According to the results of Kaplan-Meier analysis, the mean survival time of patients with high expression of LINC00320 was obviously prolonged than those with relatively low LINC00320 expressions (51.10 months vs. 38.77 months; t=2.874, $p$<0.05). Besides, the recurrence-free survival of patients with high expression of LINC00320 was found to significantly longer than those with poorly-expressed LINC00320 (47.93 months vs. 32.35 months; t=3.346, $p$<0.05) (Figure 1F-G). In addition, the expression levels of LINC00320 were detected in glioma cells, and it was observed that LINC00320 expressions in glioma cells were significantly decreased, with a more significant expression of LINC00320 in SHG-44 cell line. Hence, SHG-44 cells were selected for subsequent experimentation (Figure 1H).

## Effect of LINC00320 on Proliferation, Migration, Invasion and Apoptosis of Glioma Cells

In view of the low expressions of LINC00320 in gliomas, LINC00320 over-expression lentivirus was constructed firstly and transfected into the glioma cell line SHG-44 to determine how it specifically affects the proliferation, migration and invasion of gliomas. A significant increase in LINC00320 expression levels was detected by qRT-PCR (Figure 2A). In addition, CCK8 assay results showed that cell proliferation activity decreased significantly after LINC00320 over-expression (Figure 2B); Similarly, Transwell assay revealed that an obvious decrease in the number of migrated and invaded cells after LINC00320 over-expression (Figure 2CD). Meanwhile, flow cytometry with Annexin-V/PI double staining showed that the apoptosis rate increased significantly when LINC00320 was over-expressed (Figure 2E). Western Blot indicated that compared with Vector group, the protein expression of MMP9 decreased obviously, while that of cleaved-Caspase-3 increased significantly in LINC00320 group (Figure 2F). These findings indicated that over-expression of LINC00320 decreased glioma cell proliferation, migration and invasion, while promoted cell apoptosis.

## LINC00320 Regulated PLEKHA1 through Transcription Factor MYC

In order to elucidate the mechanism of LINC00320 involvement in the development of glioma, transcription factors in the downstream of LINC00320 predicted by lncMAP were further intersected with the differentially expressed genes in GSE15824 (Figure 3A). MYC was not only present in the triplet, but also expressed in the GSE15824 dataset. Furthermore, microarray analysis showed that MYC expression levels were significantly up-regulated in glioma (Figure 3B). Analysis of the expression patterns of MYC in TCGA and GTEx (Figure 3C) also indicated that MYC was highly-expressed in glioma. Next, the differentially expressed genes between the downstream gene of transcription factor MYC in the triplet and the result of microarray analysis were intersected (Figure 3D), and a downstream target gene with differential expression in glioma was finally obtained, namely, PLEKHA1. Subsequently, the expression of

PLEKHA1 in glioma was analyzed in GSE15824, and the results revealed that the expression of PLEKHA1 was evidently decreased in microarray analysis of GSE15824 (Figure 3E); besides, our experiment also analyzed the differential expression of PLEKHA1 in TCGA glioma database, with an obviously low expression in glioma as well (Figure 3F). The study continued to verify the expressions of MYC and PLEKHA1 in glioma samples and control tissues we collected clinically, and qRT-PCR results indicated that compared with control tissues, the mRNA expression level of MYC was up-regulated significantly, while that of PLEKHA1 was down-regulated obviously in glioma tissues ($p$<0.05) (Figure 3G-H). Further Pearson correlation analysis showed that LINC00320 was negatively-correlated with MYC in glioma tissue ($r^2$=-0.748, $p$=0.001), but positively-correlated with PLEKHA1 ($r^2$=0.795, $p$=0.001) (Figure 3I). These results suggested that LINC00320 was correlated with the expression of transcription factor MYC and PLEKHA1.

## LINC00320 Regulated the Expression of LEKHA1 by Recruiting Transcription Factor MYC

Cell verification was performed to determine the mechanism of the aforementioned LINC00320/MYC/PLEKHA1 signal axis. The location of LINC00320 and MYC in cells was firstly determined using immunofluorescence staining, and LINC00320 and MYC were found to be primarily located in the nucleus, and a few scattered in the cytoplasm (Figure 4A). Using the lncMAP database (http://bio-bigdata.hrbmu.edu.cn/LncMAP/survival.jsp), the triplet of downstream transcription factors and regulatory genes of LINC0032 in low-grade glioma were predicted (Figure 4B). Subsequent RIP experiment indicated that when LINC00320 was mutated, compared with IgG group, LINC00320-MUT group showed no MYC enrichment, while LINC00320-WT group had significantly enriched MYC compared with that in LINC00320-MUT group ($p$<0.05), suggesting that LINC00320 could be pulled-down by combining with MYC (Figure 4C). Meanwhile, based on the results of CHIP assay, analysis after precipitation showed that the primer of PLEKHA1 promoter could significantly detect the enrichment of PLEKHA1 mRNA, suggesting that MYC could bind to the promoter of PLEKHA1 (Figure 4D, $p$<0.05); besides, over-expression of LINC00320 inhibited the binding of MYC to the PLEKHA1 promoter (Figure 4E, $p$<0.05). Furthermore, dual luciferase reporter gene assay indicated that compared with the vector group, fluorescence intensity of MYC group decreased significantly in WT ($p$<0.05), and when the predicted binding site (MUT) was mutated, the fluorescence intensity did not shown significant changes ($p$>0.05) (Figure 4F). Finally, after over-expression of LINC00320 in SHG-44 cells, qRT-PCR results demonstrated that compared with the vector group, the expression levels of LINC00320 and PLEKHA1 were increased significantly in LINC00320 group. In the MYC group, MYC expression was significantly increased, while that of PLEKHA1 was significantly decreased; besides, compared with MYC group, the expressions of LINC00320 and PLEKHA1 were significantly increased in MYC+LINC00320 group (Figure 4G, $p$<0.05). These results suggested that over-expression of LINC00320 could inhibit the binding of MYC and PLEKHA.

## Effects of LINC00320/MYC/PLEKHA1 Axis on Proliferation, Migration, Invasion and Apoptosis of Glioma Cells

Our experiment further observed the effect of LINC00320/MYC/PLEKHA1 axis on the proliferation, migration, invasion and apoptosis of glioma cells. According to the results of qRT-PCR and Western blot, LINC0032 over-expression significantly promoted the expressions of LINC0032 and PLEKHA1, while the simultaneous over-expression of LINC0032 and MYC significantly promoted the expression of MYC and inhibited that of PLEKHA1. Moreover, LINC0032 over-expression combined with PLEKHA1 expression interference significantly inhibited the expression of PLEKHA1. The results of CCK8 assay demonstrated that although LINC00320 significantly reduced the proliferation and migration of cells, over-expression of MYC or interference of PLEKHA1 resulted in the reversed effect of over-expression of LINC00320, accompanied by upregulated proliferation ability of glioma cells (Figure 5A). Transwell assay further illustrated that when LINC00320 was transfected alone, the number of cells migrating and invading were significantly reduced. However, when MYC or si-PLEKHA1 were transfected simultaneously, the effect of LINC00320 could be blocked, while the number of cells migrating and invading increased, which promoted the migration and invasion of cells (Figure 5BC). Meanwhile, the results of flow cytometry with Annexin-V/PI double staining showed that LINC00320 transfection increased the proportion of apoptosis. However, co-transfection of MYC over-expression or si-PLEKHA1 with LINC00320 over-expression reversed the effect of LINC00320 and reduced the proportion of apoptosis (Figure 5D). Similarly, Western blot showed that LINC00320 reduced the expression of MMP9 and promoted that of cleaved-Caspase 3, which could be reversed after co-transfection of MYC over-expression or si-PLEKHA1 (Figure 5E). These results suggested that LINC00320 can regulate PLEKHA1 through the role of MYC and participated in the proliferation, migration and invasion of glioma cells.

### LINC00320 Regulated *in vivo* Tumorigenesis in Glioma

Mouse models of xenotransplantation were established to confirm the anti-tumor effect of LINC00320 *in vivo*, and stably expressed LINC00320 in SHG-44 cells were inoculated into mice. Tumor growth and weight of mice treated with LINC00320 were found to be lower relative to the vector group (Figure 6A-C). Western blot results demonstrated that PLEKHA1 protein expression levels were significantly up-regulated after LINC00320 treatment (Figure 6D). Immunohistochemistry showed that the positive expression of GFAP and Ki67 were significantly reduced after LINC00320 transfection (Figure 6E). These results indicated that LINC00320 can inhibit tumor growth *in vivo*.

## Discussion

To data, microRNAs or lncRNAs are hot-spots with the emergence of genetic research. A small proportion of lncRNAs have been characterized in depth, however, lncRNAs accepted and recognized to exhibit extensive roles in cellular and development processes of human disorders [37-39]. According to prior investigation, lncRNAs are also known to serve as prevalent regulators of gene expression, however, it still remains unclear with regard to the consequences of lncRNA inactivation or over-expression *in vivo* and *in vitro* generally in the development of tumors or non-tumor diseases [40, 41]. Moreover, the human brain with its heterogeneous cellular structure is a rich source of lncRNAs; yet, the functions of the majority of lncRNAs remain to be discovered. In lieu of this, the current study performed a series of experiments to

elucidate the mechanism and function of LINC00320 in the development of glioma by regulating the expression of PLEKHA1 through the transcription factor MYC.

Firstly, our study was initiated with bioinformatic prediction, which indicated that LINC00320 was implicated in the development of glioma. It has been reported that there was aberrant expression of LINC00320 in human malignancies, especially in glioma [33, 42]. Our subsequent microarray analyses identified low expression levels of LINC00320 in glioma, while the screened patient data also indicated that LINC00320 was poorly-expressed in glioma patients. Moreover, prognoses were found to be worse in glioma patients presenting with low expressions of LINC00320. After uncovering the aberrant expression of LINC00320 in gliomas, we further explored the effect of LINC00320 on proliferation, migration, invasion and apoptosis of glioma cells, with the clarification of intrinsic mechanism of action. To our surprise, cell proliferation activity and the number of cell migration and invasion were significantly decreased, while the apoptosis rate exhibited a marked increase after over-expression of LINC00320.Together, these findings suggested that over-expression of LINC00320 may function positively on the progression of glioma.

Furthermore, our findings demonstrated that LINC00320 regulated PLEKHA1 through the transcription factor MYC, which indicated that LINC00320 could play a role in the development of glioma by regulating the expression of PLEKHA1 through MYC. Additional *in vivo* cell experimentation in our study revealed that LINC00320 and MYC were primarily located in the nucleus, LINC00320 could be pulled-down by combining with MYC, and MYC could bind to the target gene PLEKHA1. The hard-done work of our peers has further indicated that MYC is a canonical stem cell factor, and is involved in the development and progression of multiple solid tumors [43-45], especially in the development of glioma [46], which can be explained by its function in modulating the role of several lncRNAs, miRNAs and proteins, etc. [47, 48]. Moreover, one particular study documented that inhibition of Myc can inhibit cell proliferation and induce apoptosis of glioma stem cells [46, 49]. Besides, our study further verified that over-expression of LINC00320 brought about an inhibitory effect on the binding of MYC to PLEKHA1.

After uncovering the potential mechanism, our study finally explored the regulation of PLEKHA1 by LINC00320 through the transcription factor MYC and its consequent effects on the proliferation, migration and invasion of glioma cells. Our findings present with their own basis and advantages. Previous studies have shown that lncRNA APTR represses the CDKN1A/p21 promoter independent of p53 to promote cell proliferation by recruiting polycomb proteins [50]. Meanwhile, knock-down of lncRNA MALAT1 was previously demonstrated to promote cell proliferation in gastric cancer cell line by recruiting the splicing factor SF2/ASF [51]. Returning to the focus of our study, down-regulated expressions levels LINC00320 have also been reported to serve as a tumor suppressor in glioma tissues; over-expression of LINC00320 could inhibit glioma cell proliferation by restraining the Wnt/β-catenin signaling pathway *via* the segregation of β-catenin and TCF4, which reiterates the significance of LINC00320 and relevant targeting in the progression of glioma [33]. More importantly, the above-mentioned evidence are in complete accordance with the current study, wherein step by step experimentation highlighted that over-expression of LINC00320 could suppress the abnormal biological process of glioma cells by recruiting

the transcription factor MYC to weaken the binding of MYC and PLEKHA1. The strength of our study lies in that *in vitro* and *in vivo* experiments were combined jointly on the basis of bioinformatic prediction. Furthermore, lncRNAs are known to function as key regulatory molecules in various fundamental cellular processes, and their deregulation is often assumed to contribute to carcinogenesis. Accordingly, intervention with LINC00320 in our study exactly provides potential research approach and clinical reference value in target therapy of human tumors on the basis of mechanism research. However, our study does present with limitations. The molecular mechanism of transcription regulation of transcription factor MYC for PLEKHA1 requires more exploration. Moreover, the sample size e is small in the literature. Besides, there is only one GSE dataset. While the strength of this article lies in that in vitro and in vivo experiments were combined jointly on the basis of bioinformatic prediction. Intervention with LINC00320 in this study exactly provides potential research approach and clinical reference value in target therapy of human tumors on the basis of mechanism research. Significantly, the innovation of this research lies in elaborating the effect of LINC00320/MYC/PLEKHA1 signaling axis on glioma.

# Conclusion

In conclusion, findings obtained in our study indicate that over-expression of LINC00320 can weaken the binding of MYC with PLEKHA1 by recruiting the transcription factor MYC, and ultimately inhibit the proliferation, migration and invasion, and promote the apoptosis of glioma. Moreover, interfering PLEKHA1 could reverse the effects of LINC00320 over-expression on glioma cells. These findings shed a new light on the potential of LINC00320 to as molecular biomarker for the clinicopathology and prognosis of glioma, which offers a novel molecular approach for the target therapy of glioma.

# List Of Abbreviations

Oct4: Octamer-binding transcription factor

Bmi1: B-lymphoma Moloney murine leukemia virus insertion region-1

lncRNAs: Long noncoding RNAs

PLEKHA1: PH domain-containing family A member 1

OS: overall survival

TV: volume of tumor

# Declarations

**Ethical Approval and Consent to participate** The current study was approved by the Ethics Committee of Liaocheng People's Hospital (Ethics Committee Approval No. 201212002), and was in accordance with the declaration of Helsinki. Signed informed consents were obtained from all participants prior to the

study. The human microglia cell line CHME-5, glioma cell line SHG-44, U251 and BT325 cells was purchased from the Cell Resource Center of Shanghai Institute of Life Sciences, Chinese Academy of Sciences and approved by the Ethics Committee of Liaocheng People's Hospital. Animal experiments were performed in strict accordance with the recommendations in the Guide for the Care and Use of Laboratory Animals of the National Institutes of Health, and all animal experimentation protocols were approved by the Institutional Animal Care and Use Committee of Liaocheng People's Hospital (No. 201306005). Extensive efforts were made to minimize the number and suffering of the included animals.

**Consent for publication** Not applicable.

**Availability of supporting data** All data generated or analysed during this study are included in this published article.

**Competing interests** The authors declare no competing financial interests.

**Funding** The research was funded by the Medical and Health Science and Technology Development Plan of Shandong Province in 2019 (No. 2019WSA13024) and the Medical Health Science and Technology Development Plan Project of Shandong Province in 2017 (No. 2017WS329).

**Authors' contributions** Jianyong Ji, Pengfei Xue and Juan Zheng performed experiments, contributed to experiment design, and assisted in data interpretation; Rongrong Li and Jinyue Fu helped design experiments and assisted in data interpretation and statistical analysis; Zhaohao Wang and Xin Li supervised planning of experiments and data interpretation and contributed to the preparation of the manuscript; Jianyong Ji wrote the manuscript. All authors read and approved the final manuscript.

**Acknowledgements** We acknowledge and appreciate our colleagues for their valuable efforts and comments on this paper.

# References

1. Alexiou G A KAP. Systemic Chemotherapy in Brain Gliomas: A Practical Atlas. Epilepsy Surgery and Intrinsic Brain Tumor Surgery. 2019
2. Jin Z, Jin RH, Ma C, Li HS, Xu HY. Serum expression level of miR-504 can differentiate between glioblastoma multiforme and solitary brain metastasis of non-small cell lung carcinoma. J BUON. 2017; 22(2)**:**474-80
3. Wu J, Neale N, Huang Y, Bai HX, Li X, Zhang Z, et al. Comparison of Adjuvant Radiation Therapy Alone and Chemotherapy Alone in Surgically Resected Low-Grade Gliomas: Survival Analyses of 2253 Cases from the National Cancer Data Base. World Neurosurg. 2018; 112(e812-e22.https://doi.org/10.1016/j.wneu.2018.01.163.
4. Di Cristofori A, Zarino B, Fanizzi C, Fornara GA, Bertani G, Rampini P, et al. Analysis of factors influencing the access to concomitant chemo-radiotherapy in elderly patients with high grade

gliomas: role of MMSE, age and tumor volume. J Neurooncol. 2017; 134(2):377-85.https://doi.org/10.1007/s11060-017-2537-2.

5. de Blank P, Bandopadhayay P, Haas-Kogan D, Fouladi M, Fangusaro J. Management of pediatric low-grade glioma. Curr Opin Pediatr. 2019; 31(1):21-7.https://doi.org/10.1097/MOP.0000000000000717.
6. Huang J, Zheng J, Yuan H, McGinnis K. Distinct tissue-specific transcriptional regulation revealed by gene regulatory networks in maize. BMC Plant Biol. 2018; 18(1):111.https://doi.org/10.1186/s12870-018-1329-y.
7. Songdej N, Rao AK. Hematopoietic transcription factor mutations: important players in inherited platelet defects. Blood. 2017; 129(21):2873-81.https://doi.org/10.1182/blood-2016-11-709881.
8. Vadde BVL, Challa KR, Nath U. The TCP4 transcription factor regulates trichome cell differentiation by directly activating GLABROUS INFLORESCENCE STEMS in Arabidopsis thaliana. Plant J. 2018; 93(2):259-69.https://doi.org/10.1111/tpj.13772.
9. Gaarenstroom T, Hill CS. TGF-beta signaling to chromatin: how Smads regulate transcription during self-renewal and differentiation. Semin Cell Dev Biol. 2014; 32(107-18.https://doi.org/10.1016/j.semcdb.2014.01.009.
10. Wu Y, Guo Z, Wu H, Wang X, Yang L, Shi X, et al. SUMOylation represses Nanog expression via modulating transcription factors Oct4 and Sox2. PLoS One. 2012; 7(6):e39606.https://doi.org/10.1371/journal.pone.0039606.
11. Qian X, Kim JK, Tong W, Villa-Diaz LG, Krebsbach PH. DPPA5 Supports Pluripotency and Reprogramming by Regulating NANOG Turnover. Stem Cells. 2016; 34(3):588-600.https://doi.org/10.1002/stem.2252.
12. Zhang XY, Ma ZP, Cui WL, Pang XL, Chen R, Wang L, et al. [Impact of PRDM1 gene inactivation on C-MYC regulation in diffuse large B-cell lymphoma]. Zhonghua Bing Li Xue Za Zhi. 2018; 47(1):25-31.https://doi.org/10.3760/cma.j.issn.0529-5807.2018.01.006.
13. Paglia S, Sollazzo M, Di Giacomo S, Strocchi S, Grifoni D. Exploring MYC relevance to cancer biology from the perspective of cell competition. Semin Cancer Biol. 2020; 63(49-59.https://doi.org/10.1016/j.semcancer.2019.05.009.
14. Trop-Steinberg S, Azar Y. Is Myc an Important Biomarker? Myc Expression in Immune Disorders and Cancer. Am J Med Sci. 2018; 355(1):67-75.https://doi.org/10.1016/j.amjms.2017.06.007.
15. Bragelmann J, Bohm S, Guthrie MR, Mollaoglu G, Oliver TG, Sos ML. Family matters: How MYC family oncogenes impact small cell lung cancer. Cell Cycle. 2017; 16(16):1489-98.https://doi.org/10.1080/15384101.2017.1339849.
16. Fallah Y, Brundage J, Allegakoen P, Shajahan-Haq AN. MYC-Driven Pathways in Breast Cancer Subtypes. Biomolecules. 2017; 7(3).https://doi.org/10.3390/biom7030053.
17. Stine ZE, Walton ZE, Altman BJ, Hsieh AL, Dang CV. MYC, Metabolism, and Cancer. Cancer Discov. 2015; 5(10):1024-39.https://doi.org/10.1158/2159-8290.CD-15-0507.
18. Berger A, Brady NJ, Bareja R, Robinson B, Conteduca V, Augello MA, et al. N-Myc-mediated epigenetic reprogramming drives lineage plasticity in advanced prostate cancer. J Clin Invest. 2019;

129(9):3924-40.https://doi.org/10.1172/JCI127961.

19. Shi J, Li YM, Fang XD. The mechanism and clinical significance of long noncoding RNA-mediated gene expression via nuclear architecture. Yi Chuan. 2017; 39(3):189-99.https://doi.org/10.16288/j.yczz.16-385.
20. Guo X, Hua Y. CCAT1: an oncogenic long noncoding RNA in human cancers. J Cancer Res Clin Oncol. 2017; 143(4):555-62.https://doi.org/10.1007/s00432-016-2268-3.
21. Yu X, Cao Y, Tang L, Yang Y, Chen F, Xia J. Baicalein inhibits breast cancer growth via activating a novel isoform of the long noncoding RNA PAX8-AS1-N. J Cell Biochem. 2018; 119(8):6842-56.https://doi.org/10.1002/jcb.26881.
22. Scacalossi KR, van Solingen C, Moore KJ. Long non-coding RNAs regulating macrophage functions in homeostasis and disease. Vascul Pharmacol. 2019; 114(122-30.https://doi.org/10.1016/j.vph.2018.02.011.
23. Liu K, Mao X, Chen Y, Li T, Ton H. Regulatory role of long non-coding RNAs during reproductive disease. Am J Transl Res. 2018; 10(1):1-12
24. Tasharrofi B, Ghafouri-Fard S. Long Non-coding RNAs as Regulators of the Mitogen-activated Protein Kinase (MAPK) Pathway in Cancer. Klin Onkol. 31(2):95-102.https://doi.org/10.14735/amko201895.
25. Fan S, Fan C, Liu N, Huang K, Fang X, Wang K. Downregulation of the long non-coding RNA ZFAS1 is associated with cell proliferation, migration and invasion in breast cancer. Mol Med Rep. 2018; 17(5):6405-12.https://doi.org/10.3892/mmr.2018.8707.
26. Fu LL, Li CJ, Xu Y, Li LY, Zhou X, Li DD, et al. Role of lncRNAs as Novel Biomarkers and Therapeutic Targets in Ovarian Cancer. Crit Rev Eukaryot Gene Expr. 2017; 27(2):183-95.https://doi.org/10.1615/CritRevEukaryotGeneExpr.2017019244.
27. Li S, Yang J, Xia Y, Fan Q, Yang KP. Long Noncoding RNA NEAT1 Promotes Proliferation and Invasion via Targeting miR-181a-5p in Non-Small Cell Lung Cancer. Oncol Res. 2018; 26(2):289-96.https://doi.org/10.3727/096504017X15009404458675.
28. Chen H, Li Q, Liang J, Jin M, Lu A. LncRNA CPS1-IT1 serves as anti-oncogenic role in glioma. Biomed Pharmacother. 2019; 118(109277.https://doi.org/10.1016/j.biopha.2019.109277.
29. Tang J, Yu B, Li Y, Zhang W, Alvarez AA, Hu B, et al. TGF-beta-activated lncRNA LINC00115 is a critical regulator of glioma stem-like cell tumorigenicity. EMBO Rep. 2019; 20(12):e48170.https://doi.org/10.15252/embr.201948170.
30. Li Z, Tan H, Zhao W, Xu Y, Zhang Z, Wang M, et al. Integrative analysis of DNA methylation and gene expression profiles identifies MIR4435-2HG as an oncogenic lncRNA for glioma progression. Gene. 2019; 715(144012.https://doi.org/10.1016/j.gene.2019.144012.
31. Zhou XY, Liu H, Ding ZB, Xi HP, Wang GW. lncRNA SNHG16 Exerts Oncogenic Functions in Promoting Proliferation of Glioma Through Suppressing p21. Pathol Oncol Res. 2020; 26(2):1021-8.https://doi.org/10.1007/s12253-019-00648-7.
32. Mills JD, Chen J, Kim WS, Waters PD, Prabowo AS, Aronica E, et al. Long intervening non-coding RNA 00320 is human brain-specific and highly expressed in the cortical white matter. Neurogenetics.

2015; 16(3):201-13.https://doi.org/10.1007/s10048-015-0445-1.

33. Tian S, Liu W, Pan Y, Zhan S. Long non-coding RNA Linc00320 inhibits glioma cell proliferation through restraining Wnt/beta-catenin signaling. Biochem Biophys Res Commun. 2019; 508(2):458-64.https://doi.org/10.1016/j.bbrc.2018.11.101.
34. Lu J, Wu QQ, Zhou YB, Zhang KH, Pang BX, Li L, et al. Cancer Research Advance in CKLF-like MARVEL Transmembrane Domain Containing Member Family (Review). Asian Pac J Cancer Prev. 2016; 17(6):2741-4
35. Hu Y, Tan LJ, Chen XD, Greenbaum J, Deng HW. Identification of novel variants associated with osteoporosis, type 2 diabetes and potentially pleiotropic loci using pleiotropic cFDR method. Bone. 2018; 117(6-14.https://doi.org/10.1016/j.bone.2018.08.020.
36. Gupta S, Iljin K, Sara H, Mpindi JP, Mirtti T, Vainio P, et al. FZD4 as a mediator of ERG oncogene-induced WNT signaling and epithelial-to-mesenchymal transition in human prostate cancer cells. Cancer Res. 2010; 70(17):6735-45.https://doi.org/10.1158/0008-5472.CAN-10-0244.
37. Panir K, Schjenken JE, Robertson SA, Hull ML. Non-coding RNAs in endometriosis: a narrative review. Hum Reprod Update. 2018; 24(4):497-515.https://doi.org/10.1093/humupd/dmy014.
38. Cui H, Banerjee S, Guo S, Xie N, Ge J, Jiang D, et al. Long noncoding RNA Malat1 regulates differential activation of macrophages and response to lung injury. JCI Insight. 2019; 4(4).https://doi.org/10.1172/jci.insight.124522.
39. D'Haene E, Jacobs EZ, Volders PJ, De Meyer T, Menten B, Vergult S. Identification of long non-coding RNAs involved in neuronal development and intellectual disability. Sci Rep. 2016; 6(28396.https://doi.org/10.1038/srep28396.
40. Liang Y, Chen X, Wu Y, Li J, Zhang S, Wang K, et al. LncRNA CASC9 promotes esophageal squamous cell carcinoma metastasis through upregulating LAMC2 expression by interacting with the CREB-binding protein. Cell Death Differ. 2018; 25(11):1980-95.https://doi.org/10.1038/s41418-018-0084-9.
41. Dolcino M, Pelosi A, Fiore PF, Patuzzo G, Tinazzi E, Lunardi C, et al. Long Non-Coding RNAs Play a Role in the Pathogenesis of Psoriatic Arthritis by Regulating MicroRNAs and Genes Involved in Inflammation and Metabolic Syndrome. Front Immunol. 2018; 9(1533.https://doi.org/10.3389/fimmu.2018.01533.
42. Dong Y, Zhang T, Li X, Yu F, Guo Y. Comprehensive analysis of coexpressed long noncoding RNAs and genes in breast cancer. J Obstet Gynaecol Res. 2019; 45(2):428-37.https://doi.org/10.1111/jog.13840.
43. Wang X, Huang Z, Wu Q, Prager BC, Mack SC, Yang K, et al. MYC-Regulated Mevalonate Metabolism Maintains Brain Tumor-Initiating Cells. Cancer Res. 2017; 77(18):4947-60.https://doi.org/10.1158/0008-5472.CAN-17-0114.
44. Rickman DS, Schulte JH, Eilers M. The Expanding World of N-MYC-Driven Tumors. Cancer Discov. 2018; 8(2):150-63.https://doi.org/10.1158/2159-8290.CD-17-0273.
45. Wahlstrom T, Henriksson MA. Impact of MYC in regulation of tumor cell metabolism. Biochim Biophys Acta. 2015; 1849(5):563-9.https://doi.org/10.1016/j.bbagrm.2014.07.004.

46. Higuchi F, Fink AL, Kiyokawa J, Miller JJ, Koerner MVA, Cahill DP, et al. PLK1 Inhibition Targets Myc-Activated Malignant Glioma Cells Irrespective of Mismatch Repair Deficiency-Mediated Acquired Resistance to Temozolomide. Mol Cancer Ther. 2018; 17(12):2551-63.https://doi.org/10.1158/1535-7163.MCT-18-0177.
47. Yi R, Feng J, Yang S, Huang X, Liao Y, Hu Z, et al. miR-484/MAP2/c-Myc-positive regulatory loop in glioma promotes tumor-initiating properties through ERK1/2 signaling. J Mol Histol. 2018; 49(2):209-18.https://doi.org/10.1007/s10735-018-9760-9.
48. Zhang G, Dong Z, Prager BC, Kim LJ, Wu Q, Gimple RC, et al. Chromatin remodeler HELLS maintains glioma stem cells through E2F3 and MYC. JCI Insight. 2019; 4(7).https://doi.org/10.1172/jci.insight.126140.
49. Chen X, Yang F, Zhang T, Wang W, Xi W, Li Y, et al. MiR-9 promotes tumorigenesis and angiogenesis and is activated by MYC and OCT4 in human glioma. J Exp Clin Cancer Res. 2019; 38(1):99.https://doi.org/10.1186/s13046-019-1078-2.
50. Negishi M, Wongpalee SP, Sarkar S, Park J, Lee KY, Shibata Y, et al. A new lncRNA, APTR, associates with and represses the CDKN1A/p21 promoter by recruiting polycomb proteins. PLoS One. 2014; 9(4):e95216.https://doi.org/10.1371/journal.pone.0095216.
51. Wang J, Su L, Chen X, Li P, Cai Q, Yu B, et al. MALAT1 promotes cell proliferation in gastric cancer by recruiting SF2/ASF. Biomed Pharmacother. 2014; 68(5):557-64.https://doi.org/10.1016/j.biopha.2014.04.007.

# Tables

Table 1 Sequences of primers

| Gene name | Primer sequence |
|---|---|
| LINC00320-Hsa | F: 5'-GACTCCTTTGGGAGACCAGTG-3' |
| | R: 5'-AGGTCACAGGGGATTTGATGG-3' |
| MYC-Hsa | F: 5'- GGAGGCTATTCTGCCCATTTG -3' |
| | R: 5'-CATCACCTTTTGGTCGTCGGAG-3' |
| PLEKHA1-Hsa | F: 5'-CCGGAATTCGACATGGGGCTTAAGATGTCC-3' |
| | R: 5'-CCGCTCGAGGGCTTCTGGGTCGATTTCTCC-3' |
| β-actin-Hsa | F: 5'-GGCGACGAGGCCCAGA-3' |
| | R: 5'-CGATTTCCCGCTCGGC-3' |

Table 2 The expression of LINC00320

| | | Low expression (n=31) | High expression (n=29) | |
|---|---|---|---|---|
| Gender | | | | 0.5933 |
| Male | 38 | 21 | 17 | |
| Female | 22 | 10 | 12 | |
| Age | | | | 0.1699 |
| ≤55 | 35 | 17 | 18 | |
| >55 | 25 | 14 | 11 | |
| Tumor size | | | | 0.0164 |
| ≤5 | 45 | 19 | 26 | |
| >5 | 15 | 12 | 3 | |
| Stage | | | | < 0.0001 |
| I~II | 31 | 7 | 24 | |
| III | 29 | 24 | 5 | |
| KHO stage | | | | 0.0098 |
| I~II | 35 | 13 | 22 | |
| III | 25 | 18 | 7 | |
| KPS score | | | | 0.0026 |
| ≥80 | 21 | 5 | 16 | |
| <80 | 39 | 26 | 13 | |
| Recurrence or not | | | | 0.1094 |
| With | 21 | 14 | 7 | |
| Without | 39 | 17 | 22 | |

# Figures

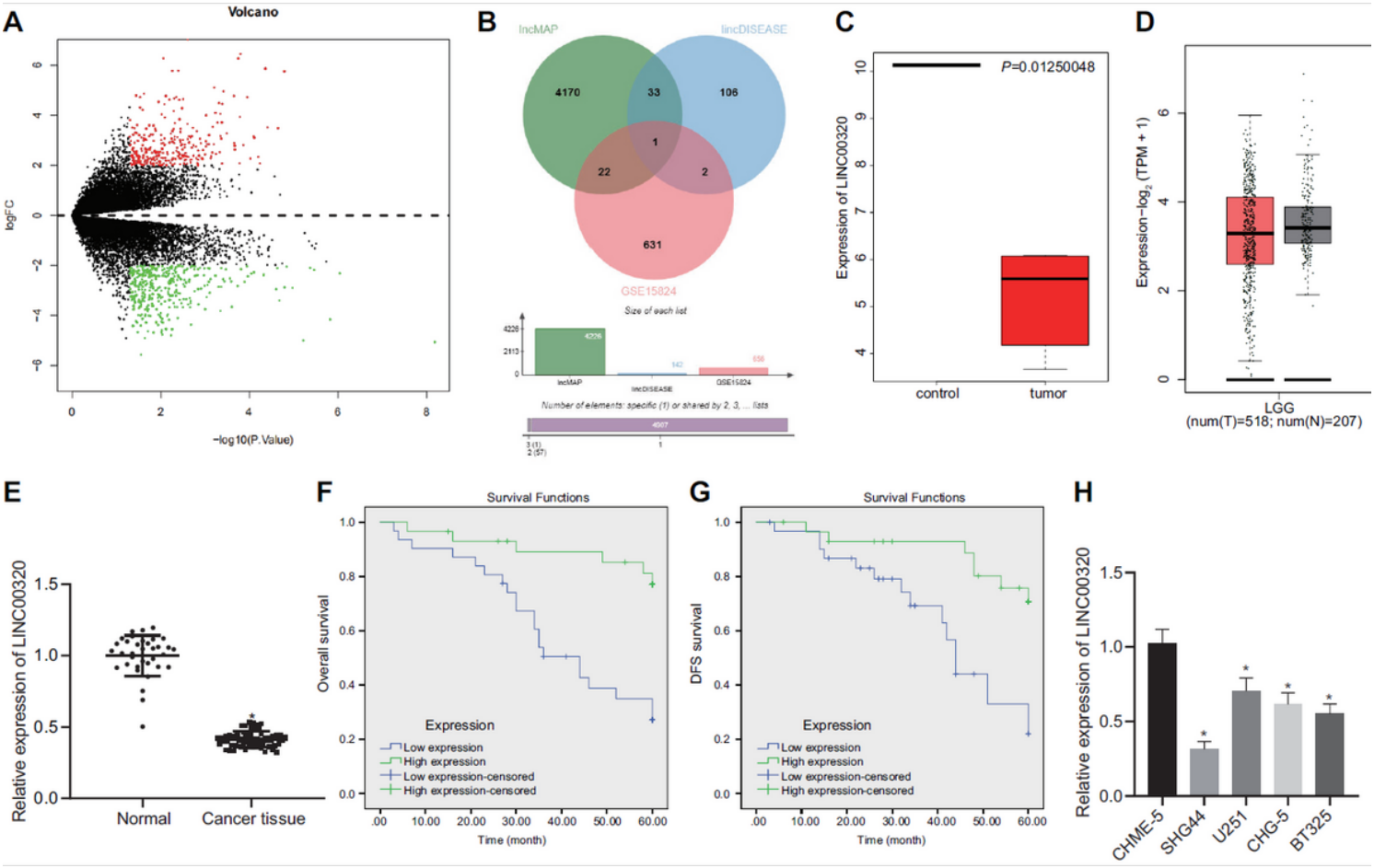


## Figure 1

LINC00320 involved in the development of glioma Note: A: Chip GSE15824 differential gene volcano map, abscissa represents -log10(p value), and ordinate represents logFC; Each point in the figure represents a gene, the green point represents a gene significantly under expressed in the disease, and the red point represents a gene significantly overexpressed in the disease. B: Prediction of lncRNAs with significant different expression in GSE15824 and glioma related lncRNAs in LINCDESEASE database, and intersection of prediction results of lncRNA triplets related to low grade glioma in lncMAP. The middle part represents the intersection of three groups of data. C: The differential expression of candidate lncRNAs in GSE15824 chip. The abscissa represents the lncRNA name, the ordinate represents the expression value, the left side represents the normal sample, and the red box plot on the right represents the disease sample. D: Expression of LINC00320 in low-grade glioma within TCGA database. The red box diagram shows tumor samples and the gray box diagram shows normal samples. E: qRT-PCR analysis showed that LINC00320 was significantly lowly expressed in glioma. F: Kaplan-Meier analysis of the relationship between LINC00320 expression and the survival of patients. G: Kaplan-Meier analysis of the relationship between LINC00320 expression and recurrence-free survival of patients; H: qRT-PCR detection of the expression level of LINC00320 in glioma cells. *compared with control group or CHME-5 group, $p<0.05$.

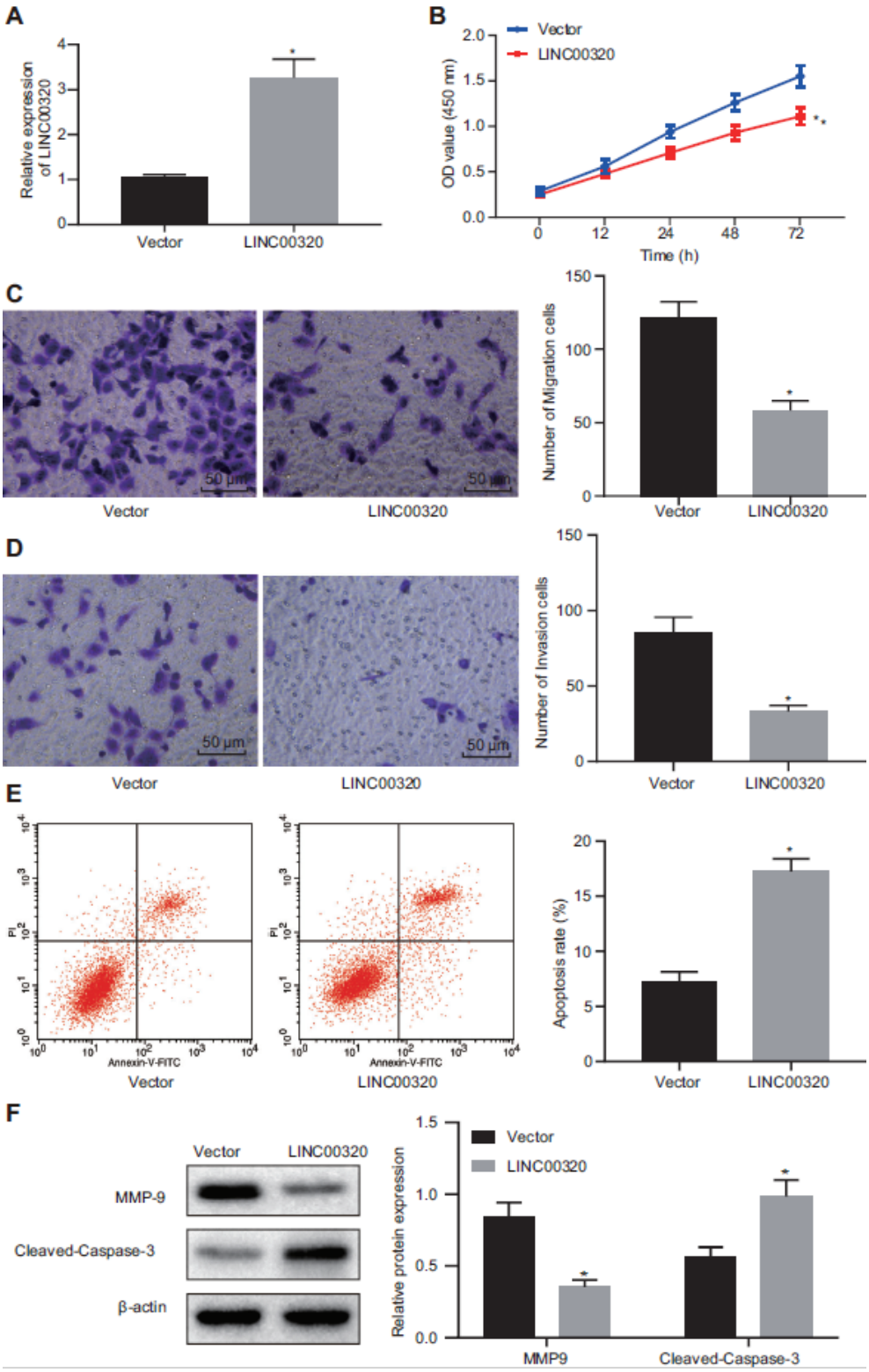


## Figure 2

Effects of LINC00320 on proliferation, migration, invasion and apoptosis of glioma cells Note: A: qRT-PCR analysis showed LINC00320 was significantly highly expressed in glioma following over-expression of LINC00320. B: CCK8 assay showed that LINC00320 inhibited the proliferation of glioma cells. C: Transwell assay indicated that LINC00320 over-expression reduced cell migration. D: Transwell assay indicated that LINC00320 over-expression reduced cell invasion. E: Annexin-V/PI flow cytometry showed

that the apoptotic rate of overexpressed LINC00320 cells was significantly up-regulated. F: Western blot detection of protein expression. The data were expressed as mean ± standard deviation, and t-est test was used to analyze the data between groups, *compared with vector group, p<0.05,

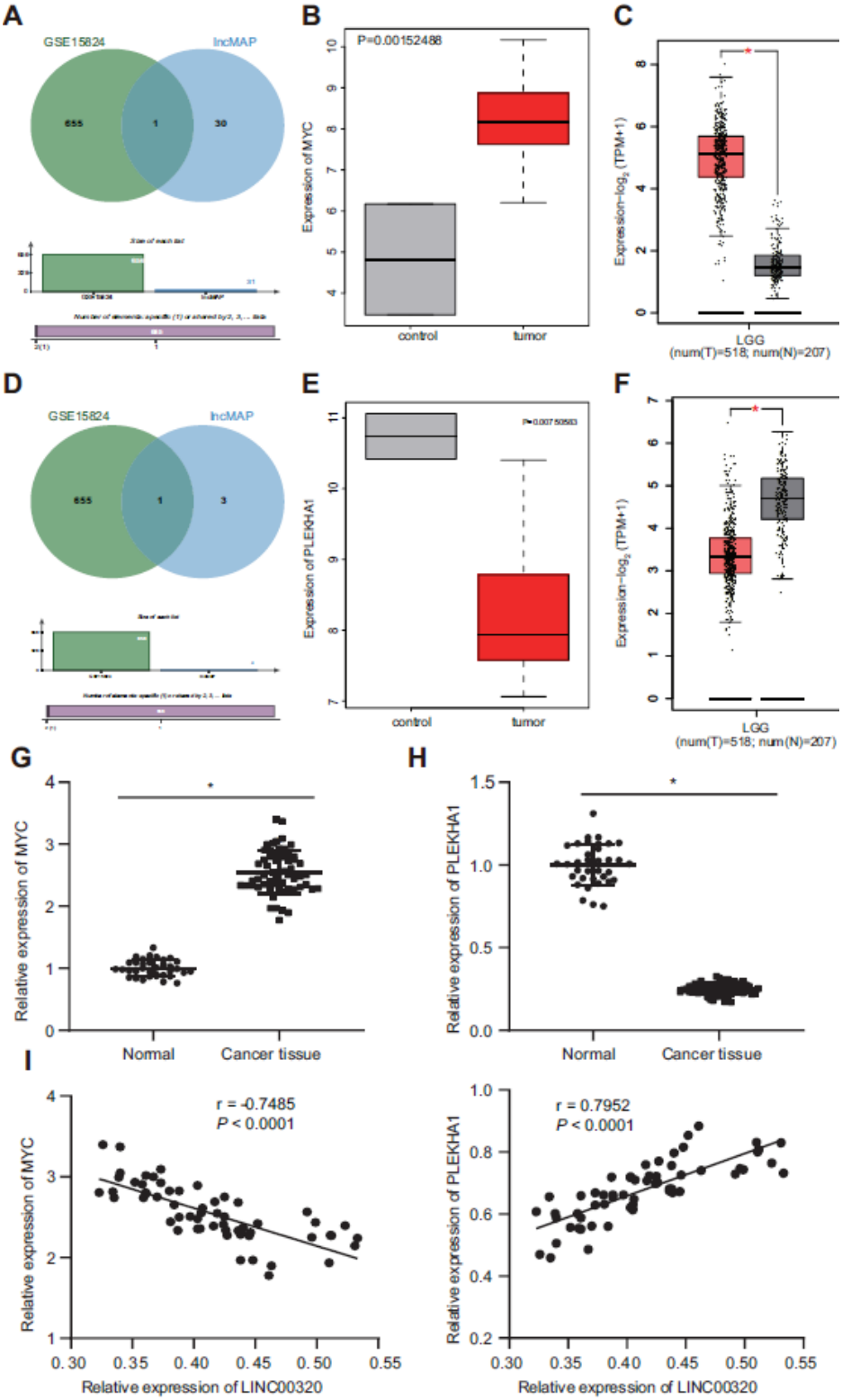


## Figure 3

The presence of correlation in the LINC00320/MYC/PLEKHA1 axis in glioma Note: A: The predicted results of transcription factors in the downstream of lncRNA and the intersection of differential expressed

genes in GSE15824 chip. B: The differential expression of candidate genes in GSE15824 chip. C: The differential expression of transcription factor MYC in low-grade gliomas predicted by TCGA website (*: p<0.01). D: Intersection of mRNA prediction results according to the lncRNA-transcription factor-mRNA triplet results predicted by GSE15824 and lncMAP database. E: Differential expression of PLEKHA1 in GSE15824 chip. F: Differential expression of PLEKHA1 in low grade glioma within TCGA (*: p<0.01). G: qRT-PCR detection of the expression of MYC in glioma tissue. H: qRT-PCR detection of the expression of PLEKHA1 in glioma tissue. I: Pearson correlation analysis of LINC00320/MYC/PLEKHA1 in glioma tissue. The data were expressed as mean ± standard deviation, and t-est test was used to analyze the data between groups. N=128, *p<0.05.

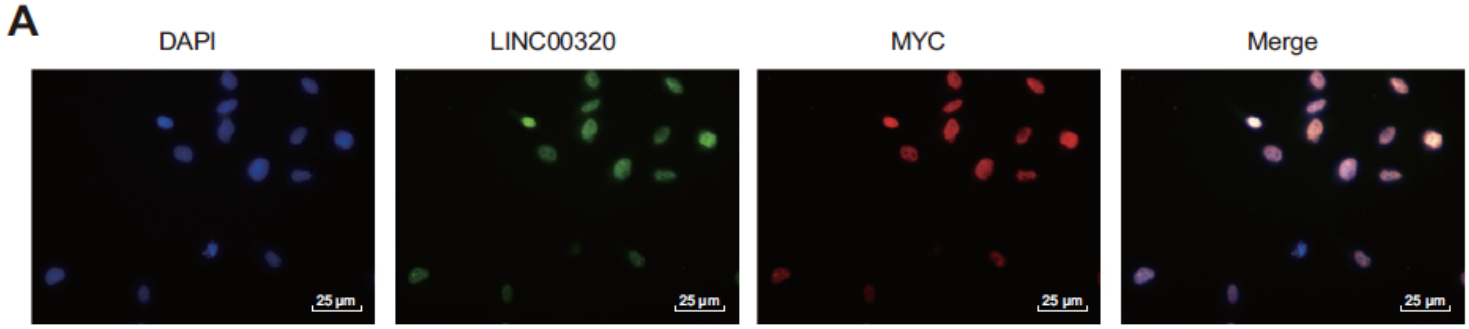


B

| Matrix ID | Name | Score | Relative Score | Sequence ID | Start | End | Strand | Predicted sequence |
|---|---|---|---|---|---|---|---|---|
| MA0147.3 | MYC | 7.69283 | 0.82845147542 | | 2003 | 2014 | + | ggacgcgtgcgc |

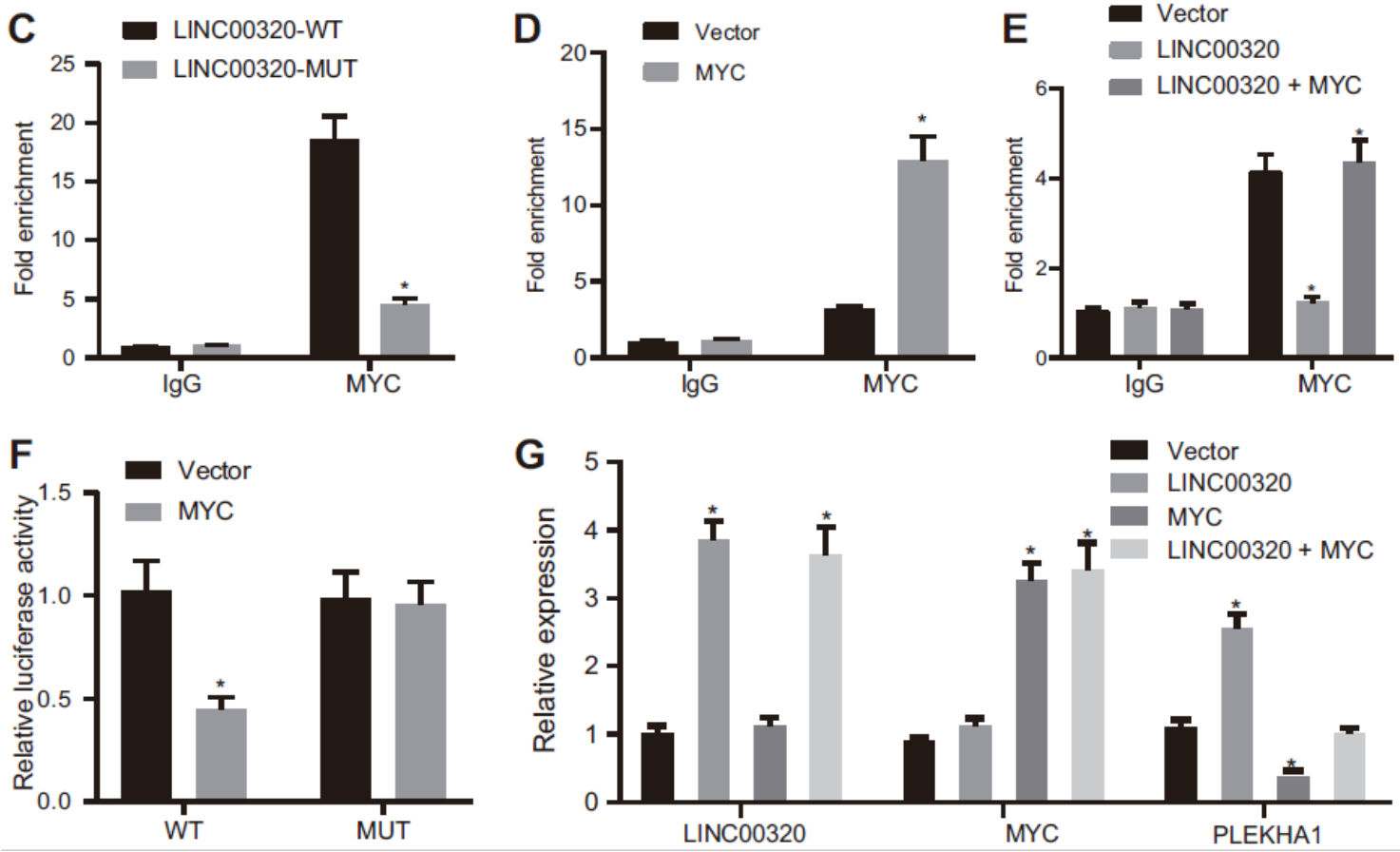

## Figure 4

Over-expression of LINC00320 inhibited the binding of MYC to PLEKHA1 Note: A: Immunofluorescence assay showed that LINC00320 and MYC were mainly located in the nucleus. B: The binding site between transcription factor and regulatory gene. C: RIP test showed that LINC00320 could bind with MYC. D: CHIP test indicated that PLEKHA1 could be enriched significantly after the complex was precipitated with MYC antibody. E: CHIP test revealed that over-expression of LINC00320 inhibited the binding of MYC with PLEKHA1. F: Dual luciferase reporter assay showed the existence of binding site between MYC and PLEKHA1. G: qRT-PCR detection of the regulation of LINC00320 and MYC on PLEKHA1 expression. The data were expressed as mean ± standard deviation, t-est test was used to analyze the data between groups, one-way ANOVA was used for statistical analysis among multiple groups, and the experiment was repeated three times. *$p<0.05$.

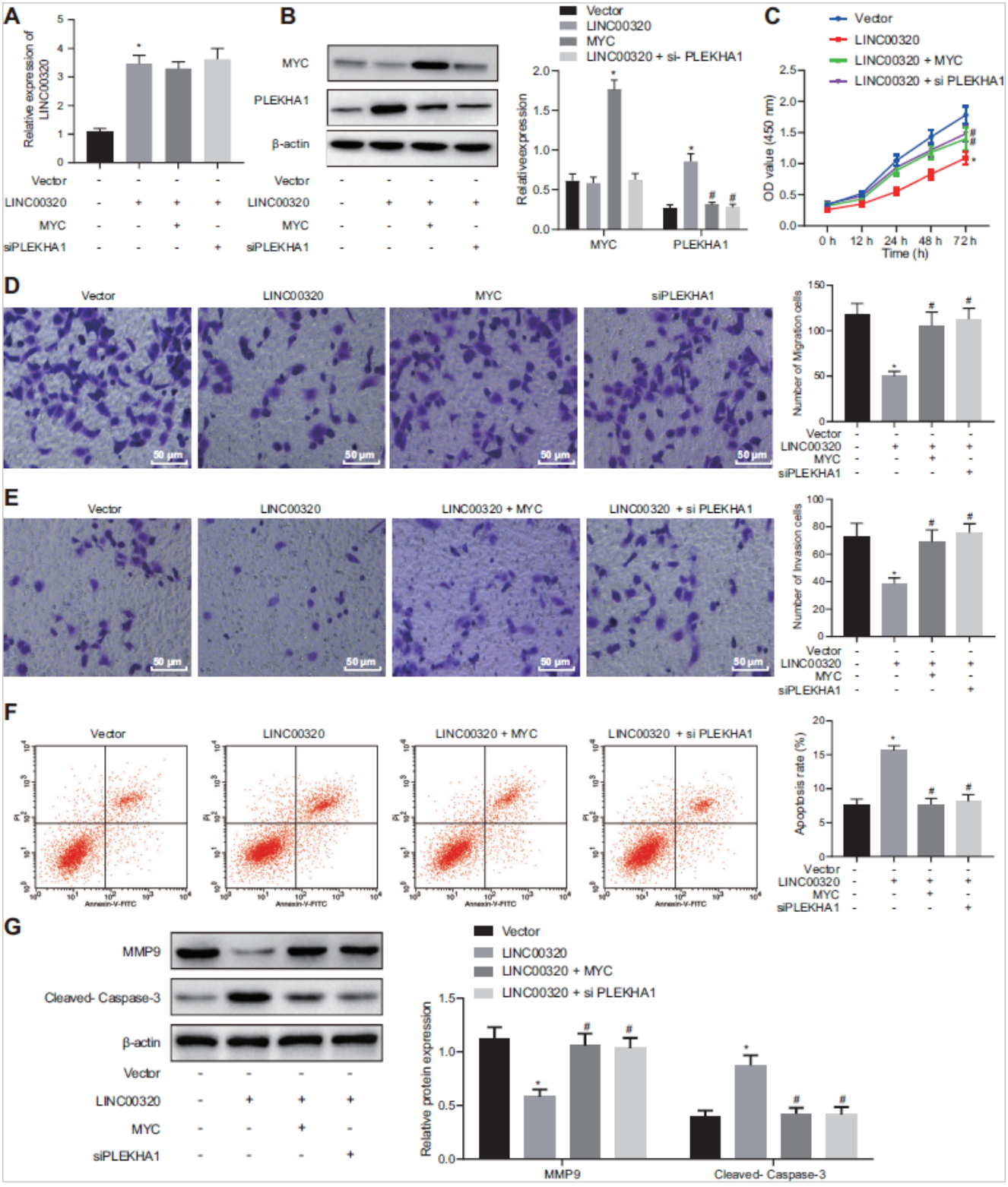


## Figure 5

LINC00320/MYC/PLEKHA1 axis involved in regulating the proliferation, migration, invasion and apoptosis of glioma cells Note: A: qRT-PCR detection of the expression of LINC00320 in different groups. B: Western blot detection of the expression of MYC/PLEKHA in different groups. C. CCK8 assay to observe the effect of MYC/PLEKHA1 on the proliferation of LINC00320 cells. D: Transwell assay to evaluate the ability of MYC/PLEKHA1 to reverse the inhibition of LINC00320 on glioma cell migration. E:

Transwell assay to evaluate the ability of MYC/PLEKHA1 to reverse the inhibition of LINC00320 on glioma cell invasion. F: Annexin-V/PI double staining to detect the effect of LINC00320/MYC/PLEKHA1 axis on apoptosis of glioma cells. G: Western blot detection of MMP9 and cleaved-Caspase 3 expression in cells. The data were expressed as mean ± standard deviation, one-way ANOVA was used for statistical analysis among multiple groups, and the experiment was repeated three times. *p<0.05.

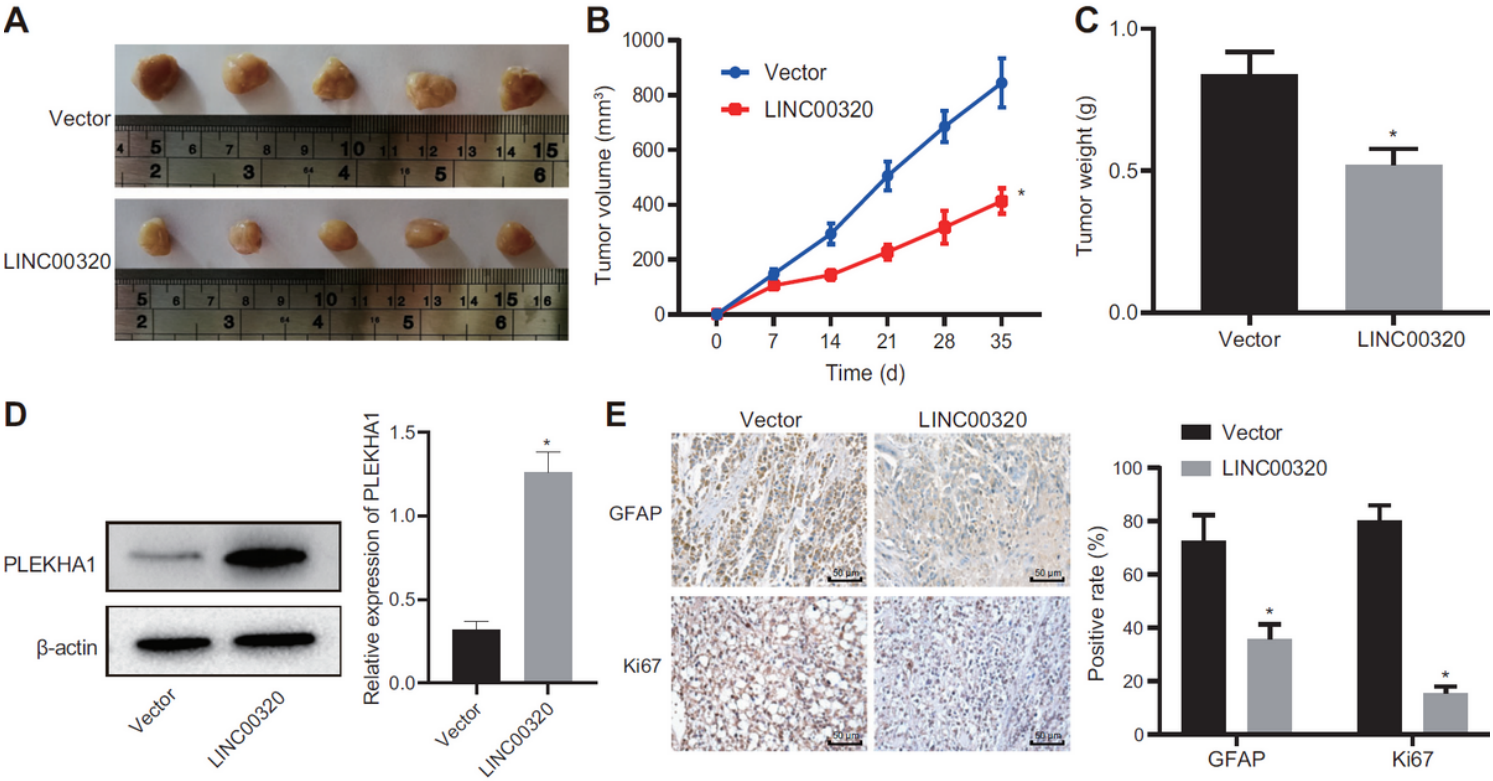


## Figure 6

LINC00320 inhibited tumor growth in nude mice Note: A: Representative image of tumor formation 35 days later; B: Statistics of tumor volume growth in nude mice; C: Tumor weight statistics of nude mice; D: Western blot detection of the expression of PLEKHA. E: Immunohistochemical observation of GFAP and Ki67 expression. The data were expressed as mean ± standard deviation, t-est test was used to analyze the data between groups, N=5, *p<0.05.